Semnan University

Progress in Physics of Applied Materials

journal homepage: https://ppam.semnan.ac.ir/

Gamma-ray and Neutron Shielding Capacity of Glasses with Various Energies and $^{241}Am-Be$ Source

H. Hosseini Sarteshnizi[a], M. Eshghi[a,*]

[a] *Department t of Physics, Imam Hossein Comprehensive University, Tehran, Iran.*

ARTICLE INFO

Article history:
Received: 30 January 2024
Revised: 24 April 2024
Accepted: 6 May 2024

Keywords:
Geant4
$^{241}Am-Be$ source
Shielding Radiation
Glass

ABSTRACT

In this research, we have investigated features of the ionizing radiation shielding of glasses, $PbO-Al_2O_3-B_2O_3-SiO_2-Bi_2O_3$, in the photon energy of 15 keV to 15 MeV. We have calculated mass attenuation coefficient (MAC) by using the Monte Carlo simulations such as Geant4 tool, XMuDat and XCOM computing programs. In the continuation of the investigation of the protection feature, we have obtained the linear attenuation coefficient (LAC), half-value layer (HVL), tenth-value layer (TVL), and mean free path (MFP). The photon flux passing through the samples in different thicknesses of chosen materials in front of the $^{241}Am-Be$ radioactive source has been shown. At the end, the energy spectrum of neutrons passing have been shown through selected samples and the ratio of transiting neutrons in the presence of samples to the ratio of transiting neutrons in the absence of selected samples and in different thicknesses.

1. Introduction

Today, nuclear radiation has many applications in medicine, industry, agriculture, etc. These rays can cause irreparable devastation to living beings and the environment. However, many people deal with these rays in various fields. Therefore, it is necessary to build shields to prevent and reduce damage caused by nuclear radiation. One of the most widely used nuclear radiation is gamma rays. Gamma rays interact with atoms and molecules in materials, depositing energy and causing. The four interactions of Rayleigh scattering, photoelectric absorption, Compton scattering, and pair production play an essential role in the fate of gamma rays and cause their absorption and scattering. The interaction cross section of gamma rays with atoms and materials varies for absorption and scattering. Generally, materials with higher atomic numbers have a larger interaction cross section for gamma rays. Therefore, atoms with heavy nuclei such as lead are always considered as a protection option. Lead is one of the elements, that has a high cross-section, and it is always considered as a choice of protective material. If this element is used as a shield, despite its good physical advantages, it has disadvantages such as toxicity, fragility, and weight, which has led scientists in this field to search for a suitable alternative. In recent years, several lead replacement materials have been proposed and designed by many researchers [1-3]. Therefore, shields are designed according to the type of application of them. For example, if a wearable shield is required, it should be more flexible. In some applications, transparent shields may be required so that the user can see the location of gamma rays source. This demand can also be met by designing and manufacturing glass protectors. Glass shields have favorable characteristics, including low cost for production, medium to high density, structural stability, high mechanical, and thermal strength, and most importantly, transparency against visible rays.

The optical transparency to visible light, easy procurement and production usage of glasses cause them to become interesting for the researchers to examine and research their shielding properties. In this regard, see [4-12].

Furthermore, among all the different glass materials, borates are popular and can be good materials for glass [2,

* Corresponding author.
E-mail address: Eshgi54@gmail.com; meshghi@ihu.ac.ir.

Cite this article as:
Hosseini Sarteshnizi, H., M. Eshghia, M., 2024. Gamma-ray and Neutron Shielding Capacity of Glasses with Various Energies and $^{241}Am-Be$-Be Source. *Progress in Physics of Applied Materials*, 4(2), pp.103-108.DOI:**10.22075/PPAM.2024.33131.1088**

13, 14], due to the many features of boric acid (B_2O_3) such as very good thermal and chemical stability, low melting point, and suitable transparency [2, 15]. Also, due to the high neutron absorption cross section in boron element, it can be used as a protection against mixed neutron-gamma sources. As a result of these good features, it's widely utilized in many various composites. In addition, the pure Silicon oxide (SiO_2) glass has very good transparency to visible light and is easily constructed [1-2], but, SiO_2 glass doesn't absorb UV light. B_2O_3 and SiO_2 can develop glasses simply all on their own, and these dominant glass shapers incorporate to create a diverse and extensively used class of glasses [2, 14]. The glasses together with Bi_2O_3, PbO, and B_2O_3 were applied in radiation usage because of their great effective atomic number and thus vigorous absorption of X-ray and γ–ray.

In this work, we calculate the quantities of gamma and neutron shielding of $PbO - Al_2O_3 - B_2O_3 - SiO_2 - Bi_2O_3$ glass systems using the Geant4 simulation tool based on Table 1.

2. Theoretical of Shielding

Here, for the reader's convenience, the usual related formulae, basic shielding parameters, for gamma-ray shielding parameters are deduced as following equations [16, 17].

In narrow-beam absorption experiments without any scattering effects, the intensity of the incident photons (I_0) decreases depending on material thickness (t) and density (ρ). According to the Beer-Lambert law, we have:

$$I = I_0 e^{-\mu t} \quad (1)$$

where μ is linear attenuation coefficient. Therefore, we have

$$\mu = \frac{1}{t}\ln\left(\frac{I}{I_0}\right) \quad (2)$$

Also, for mass attenuation coefficient, we have:

$$\mu_m = \sum_i w_i (\mu/\rho)_i \quad (3)$$

where ρ is the density of element and w_i is the density of i th material.

Other quantities can also be obtained using the attenuation coefficient. Among them are, the thickness that halves the intensity of photons, $HVL\ (cm) = \frac{\ln 2}{\mu}$, and the thickness where the intensity of photons reaches 10% of its original, $TVL\ (cm) = \frac{\ln 10}{\mu}$.

Mean Free Path (MFP) is written as below:

$$MFP(cm) = \lambda = \frac{\int_0^\infty te^{-\mu x}dt}{\int_0^\infty e^{-\mu x}dt} = \frac{1}{\mu} \quad (4)$$

3. Method and Material

Table 1 shows the molecular compounds along with their weight percentage and density.

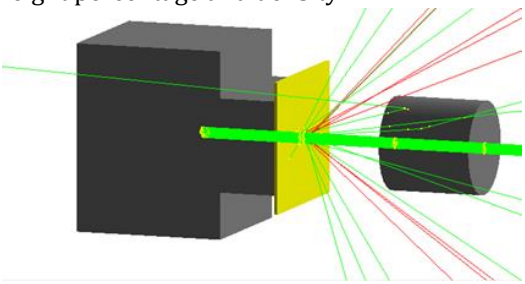

Fig. 1. Schematic of system simulation geometry by Geant4.

The simulation geometry is also shown in Figure 1. Here, the source is defined as a sphere with a diameter of 6 mm inside the lead chamber and it emits rays in the form of isotropic towards the shield marked with yellow color. At the end, the rays passed by the detector are considered sensitive. The simulations were performed using the Geant4 tools and the FTFP_BERT physics model. In order to reduce the computational error in the number of radiation particles emitted from the source, 10^7 particles were considered.

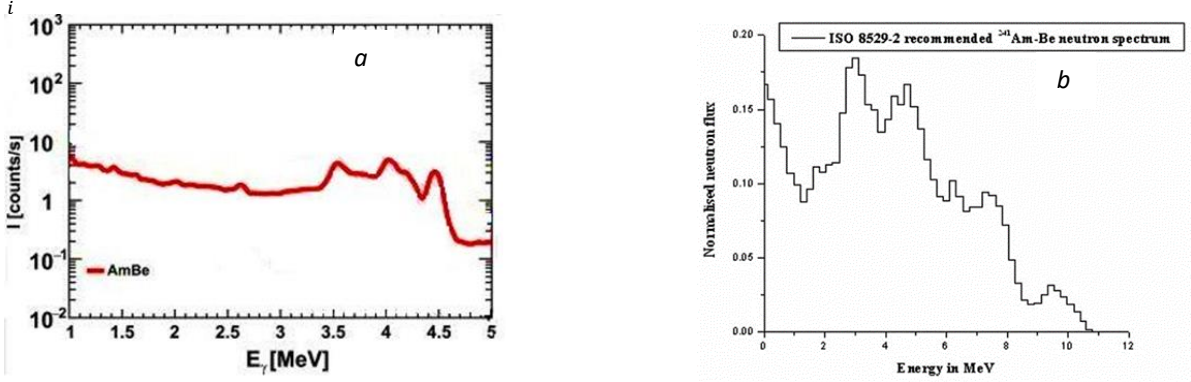

Fig. 2. *a*) Gamma spectra and *b*) neutron spectra of the ^{241}Am-Be source [18, 19].

Table1. Chemical composition and wt. fraction of elements in glasses.

Sample	PbO	Al_2O_3	B_2O_3	SiO_2	Bi_2O_3	Density (g/cm^3)
Glass1	0.10	-	0.20	0.65	0.05	3.6125
Glass2	0.25	0.1	0.65	-	-	4.3765
Glass3	0.40	0.1	0.10	0.40	-	5.5130
Glass4	0.50	0.1	-	0.40	-	6.2200
Glass5	0.30	-	0.20	-	0.50	7.8010
Glass6	0.35	-	-	0.10	0.55	8.4955

Some sources are of gamma neutron mixed type. In addition to the intensity of the transmitted photons, the intensity of the transmitted neutrons also becomes important. One of these sources is the ^{241}Am-Be source, which has gamma and neutron energy spectrum. Figure 2 shows the continuous spectrum of neutron and gamma rays for this source.

Now, we need energy histograms to define source $^{241}Am-Be$ in Geant4 tool. Based on this, we convert the spectra of Figure 2 into discrete energy histograms using Digitizer software and enter them into the Geant4 tool as a code.

4. Simulation, Discussion and Results

Using the data provided by Figure 1. we calculate the energy attenuation coefficient of glasses for the energy range of 15 keV to 15 MeV using the simulation tool of Geant4 tool, and compare them with the results obtained from XMuDat program [20] and XCOM program [21].

We have shown the results of all three simulations are presented in Figure 3 in a graph. As seen in this figure, the samples have good performance against gamma rays. In this case, denser samples have a better response to the absorption and scattering of incident photons. The presence of heavy elements such as lead and bismuth increases the absorption and scattering cross-section of photons. The corresponding K-edges of these elements are also clearly visible in Figure 3. The Glass-6 sample has the highest percentage of lead and bismuth and therefore has the best protection against gamma rays.

Also, in the continuation of our calculation work, by obtaining the flux passing through the samples and using relations 1 to 4, four coefficient quantities LAC, TVL, HVL, and MFP were also calculated and the results are shown in the form of a diagram in the Figures 4 to 7. As can be seen in those figures, photons with higher energies pass through the shields more easily, and the result is a higher transmitted flux for high-energy photons. Consequently, the linear attenuation coefficient decreases with increasing energy, while the other three quantities, i.e., TVL, HVL, and MFP increase since they are inversely related to the transmitted flux. Considering relations 1 to 4, and the dependence of quantities HVL, TVL, and MFP on the inverse of the linear attenuation coefficient, it can be seen that the behavior of HVL, TVL, and MFP graphs is the inverse of the linear attenuation coefficient graph. The presence of resonances at energies lower than 100 keV is due to the energy of the edges of K and L elements in the samples.

After the general examination of the samples against gamma photons, the protection performance of the selected samples against the $^{241}Am-Be$ source is investigated.

Now, we examine the effect of photons and neutrons passing through the samples separately. In the first case, as demonstrated in Figure 8, the flux passing through the samples due to selected source is logarithmically drawn as a function of the thickness.

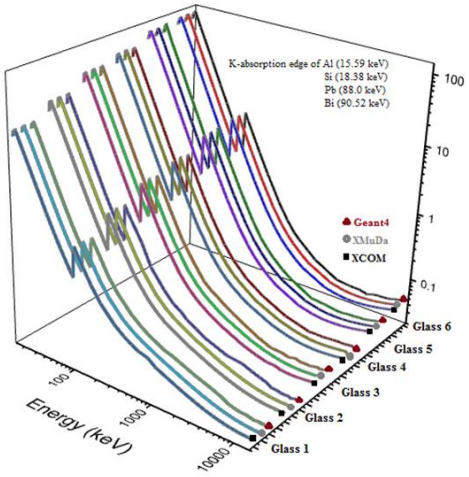

Fig. 3. Mass attenuation coefficient in terms of energy for the glass samples1 to 6 in the energy range of 15 keV to 15 MeV.

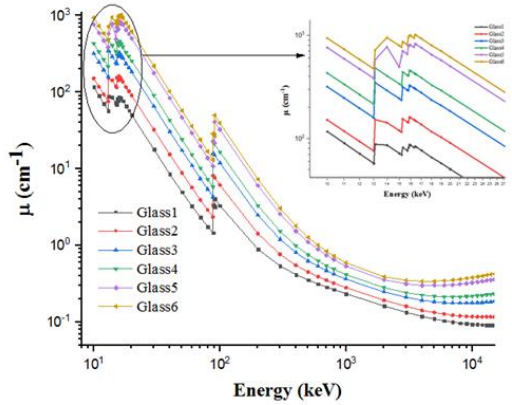

Fig. 4. Linear attenuation coefficient (LAC) in terms of energy for the glass samples1 to 6.

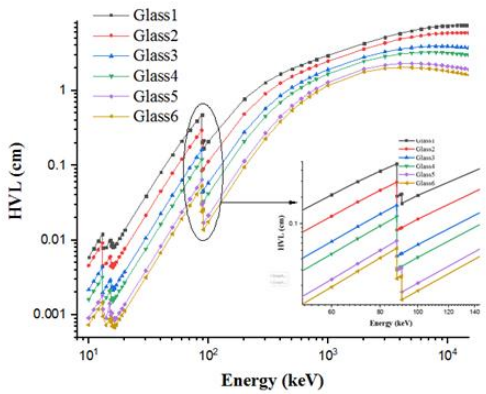

Fig. 5. The half-value layer (HVL) in terms of energy for the glass samples1 to 6.

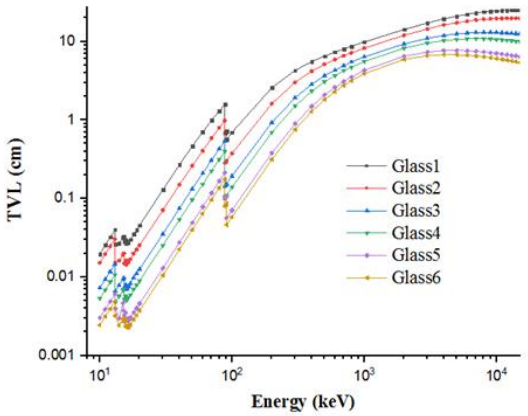

Fig. 6. The tenth-value layer (TVL) in terms of energy for the glass samples1 to 6.

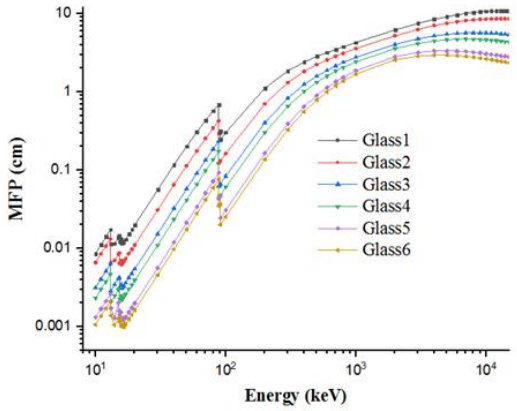

Fig. 7. The mean free path (MFP) in terms of energy for the glass samples1 to 6.

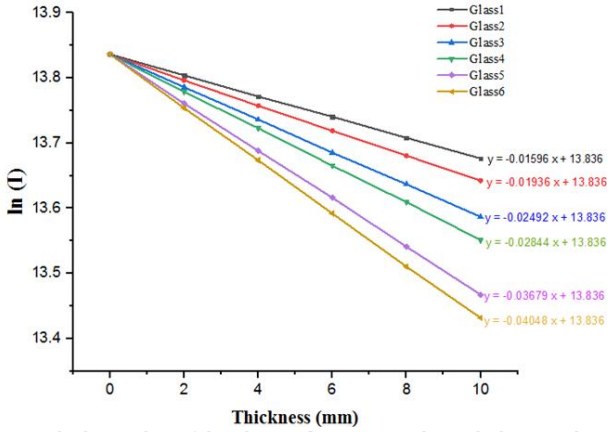

Fig. 8. The logarithm of the photon flux passing through the samples in different thicknesses in front of the ^{241}Am-Be source.

The results demonstrate that increasing the thickness of the material leads to a decrease in the intensity of transmitted photons. Figure 8 depicts the slope of each graph alongside its y-intercept, which corresponds to the initial intensity (flux) of the detected primary radiation. Due to the high concentration of bismuth and lead elements, the glass-6 sample exhibits superior performance compared to other, samples and its slope is higher too.

Also, the image of the passing flux of photons for (_ ^241) Am-Be source and Glass-1 and Glass-6 samples at a thickness of 20 mm is shown in Figure 9.

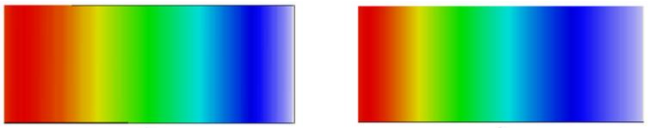

Fig. 9. The image of the flux passing through the samples a) Glass-1 and b) Glass-6 against ^{241}Am-Be source.

Here, red color means more intensity and white color means less intensity of photons. As it is clear from the pictures, the penetration power of the photon energy in sample Glass-6 is lower than that in sample Glass-1.

In the next step, we investigated the neutrons passing through the shields. The results are drawn in the form of spectrum of neutrons passing through the samples and in the form of a histogram in Figures 10.

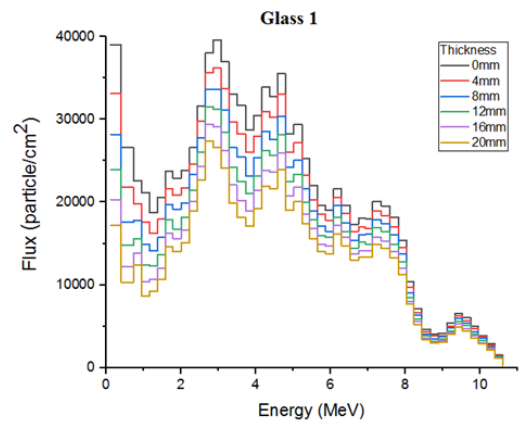

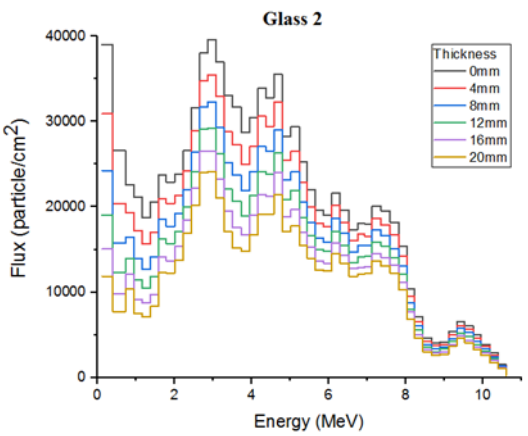

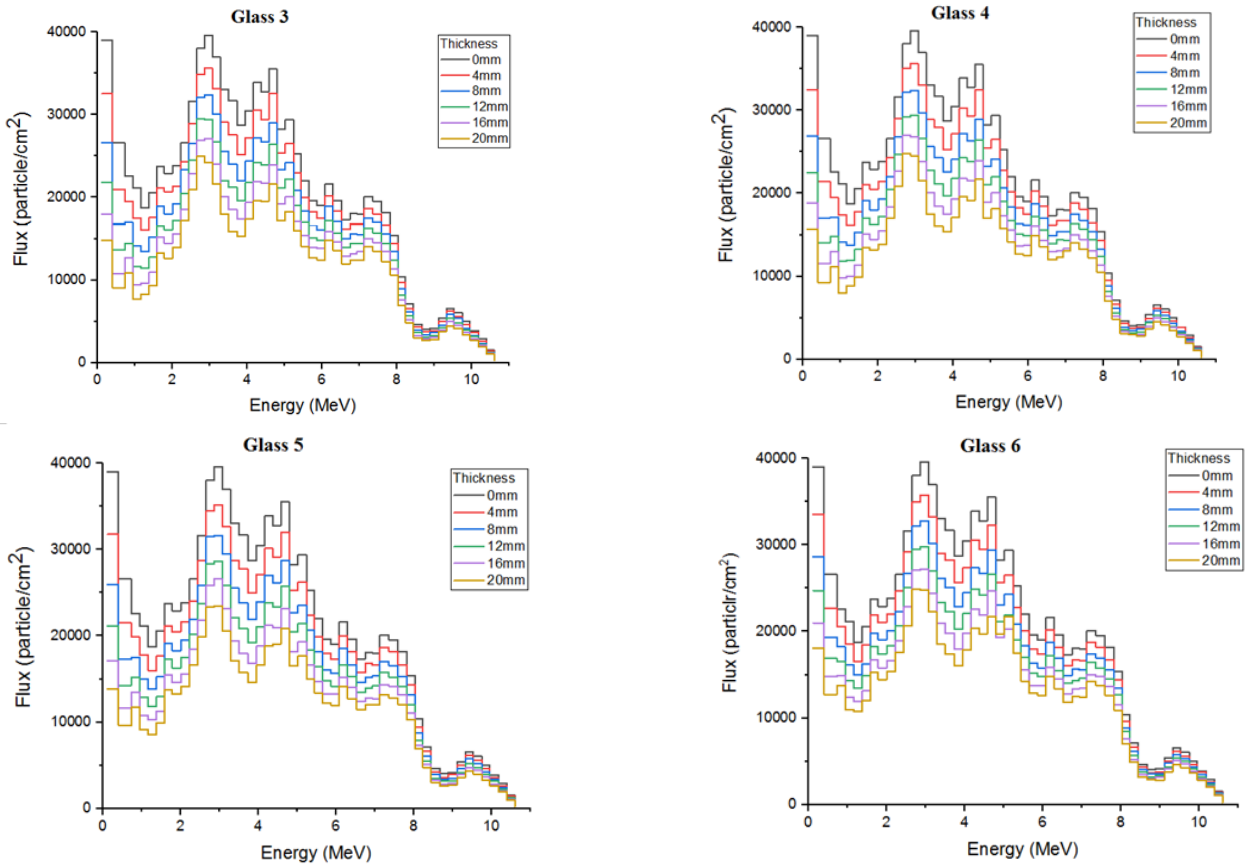

Fig. 10. Energy spectrum of neutrons passing through samples in different thicknesses.

Additionally, we can determine the shielding effectiveness of the samples by calculating the ratio of the total number of transmitted neutrons through each sample thickness to the total number of transmitted neutrons without any shielding. We have shown these ratios for any samples in Figure 11.

Figs. 10 and 11 illustrate that the neutron flux decreases with increasing the thickness of sample.

Also, the presence of element B in glass-1, glass-2, glass-3 and glass-5 samples with different weight percentages makes these samples show better performance against the reduction of intensity of passing neutrons. The glass-2 and glass-5 have the highest weight percentage of B_2O_3 molecules, 65% and 25%, respectively. Therefore, the neutron attenuation of these samples is more favorable than other samples. Because, the boron element has a high cross section against the absorption of neutrons. In glass-6, it can be seen that, contrary to the high density, it has a weaker performance than the lighter samples, and the reason is the absence of B_2O_3 molecules in this shield.

In addition, by calculating the transmission spectrum of the samples, it is possible to understand in which range of energy the shields perform better. The cross section of the neutron absorption in the element, especially the boron element, decreases with the increase of the incident neutron energy. Therefore, we expect to have more neutron absorption at low energies, which can be understood from Figures 10. Here, we see a greater distance between the spectra at low energies, which decreases with increasing energy.

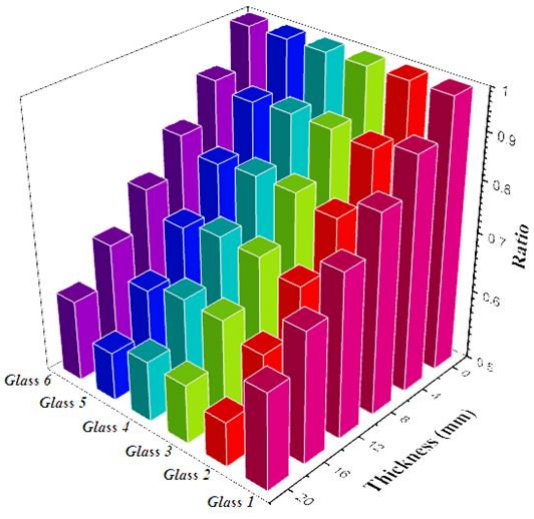

Fig. 11. The ratio of passing neutrons in the presence of samples to the ratio of passing neutrons in the absence of samples and in different thicknesses.

5. Conclusion

In this study, we investigated the shielding properties of ionizing radiation for selected glasses in the range of 15 keV to 15 MeV. We obtained results using Geant4 tool, and programs of XCOM and XMuDat, which are in good agreement with each other. The output results show that the samples have good performance against reducing the intensity of gamma rays and sample Glass-6, which has a

higher percentage of bismuth and lead, shows better results. Also, these samples have a good performance against the reduction of transiting neutrons, for which the $^{241}Am-Be$ source was used.

Acknowledgements

This research received no external funding.

Conflicts of Interest

The author declares that there is no conflict of interest regarding the publication of this article.

References

[1] Akman, F., Durak, R., Turhan, M.F. and Kaçal, M.R., 2015. Studies on effective atomic numbers, electron densities from mass attenuation coefficients near the K edge in some samarium compounds. *Applied Radiation and Isotopes*, *101*, pp.107-113.

[2] Akman, F., Geçibesler, I.H., Demirkol, I. and Çetin, A., 2019. Determination of effective atomic numbers and electron densities for some synthesized triazoles from the measured total mass attenuation coefficients at different energies. *Canadian Journal of Physics*, *97*(1), pp.86-92.

[3] Ambika, M.R., Nagaiah, N., Harish, V., Lokanath, N.K., Sridhar, M.A., Renukappa, N.M. and Suman, S.K., 2017. Preparation and characterisation of Isophthalic-Bi2O3 polymer composite gamma radiation shields. *Radiation Physics and Chemistry*, *130*, pp.351-358.

[4] Eshghi, M., 2020. Investigation of radiation protection features of the TeO_2–$B2O_3$–Bi_2O_3–Na_2O–$NdCl_3$ glass systems. *Journal of Materials Science: Materials in Electronics*, *31*(19), pp.16479-16497.

[5] Al-Buriahi, M.S., Arslan, H. and Tonguç, B.T., 2019. Mass attenuation coefficients, water and tissue equivalence properties of some tissues by Geant4, XCOM and experimental data. *Indian Journal of Pure & Applied Physics (IJPAP)*, *57*(6), pp.433-437.

[6] Sayyed, M.I., El-Mesady, I.A., Abouhaswa, A.S., Askin, A. and Rammah, Y.S., 2019. Comprehensive study on the structural, optical, physical and gamma photon shielding features of B2O3-Bi2O3-PbO-TiO2 glasses using WinXCOM and Geant4 code. *Journal of Molecular Structure*, *1197*, pp.656-665.

[7] Singh, K.J., Kaur, S. and Kaundal, R.S., 2014. Comparative study of gamma ray shielding and some properties of PbO–SiO_2–Al_2O_3 and Bi_2O_3–SiO_2–Al_2O_3 glass systems. *Radiation Physics and Chemistry*, *96*, pp.153-157.

[8] Singh, V.P. and Badiger, N.M., 2013. Study of mass attenuation coefficients, effective atomic numbers and electron densities of carbon steel and stainless steels. *Radioprotection*, *48*(3), pp.431-443.

[9] Al-Buriahi, M.S. and Rammah, Y.S., 2019. Investigation of the physical properties and gamma-ray shielding capability of borate glasses containing PbO, Al_2O_3 and Na_2 O. *Applied Physics A*, *125*, pp.1-8.

[10] Issa, S.A., Mostafa, A.M.A., Dong, M., Singh, V.P. and Tekin, H.O., 2018. Determining the gamma-ray parameters for BaO–ZnO–B2O3 glasses using MCNP5 code: a comparison study. *Radiation Effects and Defects in Solids*, *173*(5-6), pp.510-525.

[11] Medhat, M., 2012. Study of the mass attenuation coefficients and effective atomic numbers in some gemstones. *Journal of Radioanalytical and Nuclear Chemistry*, *293*(2), pp.555-564.

[12] Sayyed, M.I., Lakshminarayana, G., Dong, M.G., Ersundu, M.Ç., Ersundu, A.E. and Kityk, I.V., 2018. Investigation on gamma and neutron radiation shielding parameters for BaO/SrO–Bi_2O_3–B_2O_3 glasses. *Radiation Physics and Chemistry*, *145*, pp.26-33.

[13] Kaewkhao, J. and Limsuwan, P., 2010. Mass attenuation coefficients and effective atomic numbers in phosphate glass containing Bi_2O_3, PbO and BaO at 662 keV. *Nuclear Instruments and Methods in Physics Research Section A: Accelerators, Spectrometers, Detectors and Associated Equipment*, *619*(1-3), pp.295-297.

[14] Kirdsiri, K., Kaewkhao, J., Pokaipisit, A., Chewpraditkul, W. and Limsuwan, P., 2009. Gamma-rays shielding properties of xPbO:(100− x) B_2O_3 glasses system at 662 keV. *Annals of Nuclear Energy*, *36*(9), pp.1360-1365.

[15] Yasaka, P., Pattanaboonmee, N., Kim, H.J., Limkitjaroenporn, P. and Kaewkhao, J., 2014. Gamma radiation shielding and optical properties measurements of zinc bismuth borate glasses. *Annals of Nuclear energy*, *68*, pp.4-9.

[16] Yin, S., Wang, H., Wang, S., Zhang, J. and Zhu, Y., 2022. Effect of B_2O_3 on the radiation shielding performance of telluride lead glass system. *Crystals*, *12*(2), p.178.

[17] Limkitjaroenporn, P., Cheewasukhanont, W., Kothan, S. and Kaewkhao, J., 2021. Development of new high transparency Pb-free radiation shielding glass. *Integrated Ferroelectrics*, *214*(1), pp.181-204.

[18] Scherzinger, J., Al Jebali, R., Annand, J.R.M., Fissum, K.G., Hall-Wilton, R., Koufigar, S., Mauritzson, N., Messi, F., Perrey, H. and Rofors, E., 2017. A comparison of untagged gamma-ray and tagged-neutron yields from 241AmBe and 238PuBe sources. *Applied Radiation and Isotopes*, *127*, pp.98-102.

[19] Lebreton, L., Zimbal, A. and Thomas, D., 2007. Experimental comparison of 241Am–Be neutron fluence energy distributions. *Radiation protection dosimetry*, *126*(1-4), pp.3-7.

[20] Nowotny R., XMuDat: Photon Attenuation Data on PC; International, Atomic Energy Agency, Nuclear Data Services, Version 1.0.1 of August 1998; *https://www-nds.iaea.org/repor ts/nds-195.htm*.

[21] Berger, M.J.O.K., 2010. XCOM: photon cross sections database. *http://www. nist. gov/pml/data/xcom/index. cfm*.